Bioorganic & Medicinal Chemistry Letters 25 (2015) 5232–5236

Contents lists available at ScienceDirect

Bioorganic & Medicinal Chemistry Letters

journal homepage: www.elsevier.com/locate/bmcl

# Carborane-containing urea-based inhibitors of glutamate carboxypeptidase II: Synthesis and structural characterization

Sihyun Youn [a,†], Kyung Im Kim [a,†], Jakub Ptacek [b], Kiwon Ok [a], Zora Novakova [b], YunHye Kim [a], JaeHyung Koo [c], Cyril Barinka [b,*], Youngjoo Byun [a,d,*]

[a] College of Pharmacy, Korea University, 2511 Sejong-ro, Jochiwon-eup, Sejong 339-700, South Korea
[b] Institute of Biotechnology, Academy of Sciences of the Czech Republic, v.v.i., Laboratory of Structural Biology, Vídeňská 1083, 14220 Prague 4, Czech Republic
[c] Department of Brain Science, Daegu Gyeongbuk Institute of Science & Technology, 50-1 Sang-Ri, Hyeonpung-Myeon, Dalseong-Gun, Daegu 711-873, South Korea
[d] Biomedical Research Center, Korea University Guro Hospital, Korea University, Seoul, South Korea

ARTICLE INFO

*Article history:*
Received 1 July 2015
Revised 29 August 2015
Accepted 24 September 2015
Available online 26 September 2015

*Keywords:*
Carborane
Glutamate carboxypeptidase II
X-ray crystal structure

ABSTRACT

Glutamate carboxypeptidase II (GCPII) is a zinc metalloprotease on the surface of astrocytes which cleaves *N*-acetylaspartylglutamate to release *N*-acetylaspartate and glutamate. GCPII inhibitors can decrease glutamate concentration and play a protective role against apoptosis or degradation of brain neurons. Herein, we report the synthesis and structural analysis of novel carborane-based GCPII inhibitors. We determined the X-ray crystal structure of GCPII in complex with a carborane-containing inhibitor at 1.79 Å resolution. The X-ray analysis revealed that the bulky *closo*-carborane cluster is located in the spacious entrance funnel region of GCPII, indicating that the carborane cluster can be further structurally modified to identify promising lead structures of novel GCPII inhibitors.



Carboranes are icosahedral clusters consisting of 2 carbon atoms, 10 boron atoms and 12 hydrogen atoms. Due to their unique physical and chemical properties such as high lipophilicity, thermal stability and boron content, carboranes have been widely applied in medical science, material science and physical science.[1–6] In the field of medical science, carboranes have been long considered to be attractive boron-carriers for boron neutron capture therapy (BNCT) in the treatment of devastating cancers such as glioblastoma, melanoma, and head and neck cancer.[7–9] Due to high boron content, resistance to metabolism, and diverse chemical transformations, carboranes have been conjugated with targeting agents such as carbohydrates and nucleosides for BNCT.[10–16] More recently, *closo*-carboranes have been utilized as surrogates of lipophilic scaffolds for the identification and discovery of novel bioactive molecules.[17–21] The hydrophobic *closo*-carboranes have successfully replaced the cyclohexyl or phenyl ring of various nuclear receptor ligands.[22] These include the vitamin D receptor, retinoid receptor, estrogen receptor, and androgen receptor ligands.[23–27] The binding affinities of carborane-containing ligands for their respective target proteins were maintained or enhanced when the carborane cluster was introduced in place of the lipophilic moiety.[23–27]

Glutamate carboxypeptidase II (GCPII) is a type II zinc-dependent metalloprotease which catalyzes the cleavage of *N*-acetylaspartyl glutamate (NAAG) to produce *N*-acetylaspartate (NAA) and glutamate (Glu) in the brain.[28] It is also highly expressed in androgen-independent metastatic prostate cancer and is referred to as prostate-specific membrane antigen (PSMA). PSMA is now considered to be an excellent biomarker in the diagnosis of advanced prostate cancer. For the last two decades, a number of PSMA-targeted inhibitors have been successfully discovered and translated into clinical studies for the imaging and therapy of prostate cancer.[29–32] However, the obstacles present in the imaging and therapy of CNS diseases targeting GCPII in the brain due to low penetration of hydrophilic GCPII inhibitors across the blood–brain barrier (BBB), still need to be overcome.

To date, there have been very few reports on the X-ray crystal structure of carborane-containing ligands in complex with the cognate proteins, although the carborane cluster has been widely introduced into pharmacologically active molecules in drug design and medicinal chemistry.[33–37] The determined X-ray crystal structures of protein–carborane complexes are dihydrofolate reductase (DHFR) with 2,4-diamino-5-(1-*o*-carboranylmethyl)-6-methylpyrimidine (PDB ID: 2C2S),[33] HIV protease with cobalt bis(1,2-dicarbollide) (PDB ID: 1ZTZ),[34] vitamin D receptor (VDR) with (*R*)- and (*S*)-stereoisomers of carborane-based ligand (PDB ID: 3VJT),[35] and

* Corresponding authors. Tel.: +420 296 443 615; fax: +420 296 443 610 (C.B.); tel.: +82 44 860 1619; fax: +82 44 860 1607 (Y.B.).
*E-mail addresses:* cyril.barinka@ibt.cas.cz (C. Barinka), yjbyun1@korea.ac.kr (Y. Byun).
† Equal contribution.

http://dx.doi.org/10.1016/j.bmcl.2015.09.062
0960-894X/

carbonic anhydrase with 1-(sulfamido)methyl-1,2-dicarba-*closo*-dodecaborane analogs (PDB ID: 4MDG).[36,37]

X-ray structures of GCPII–ligand complexes identified two principal specificity pockets that contribute prominently to interactions between the enzyme and its inhibitors/substrates. The S1′ (or pharmacophore) pocket serves as a glutamate-recognition site ensuring high specificity as well as affinity for glutamate-containing small-molecules that serve as GCPII-specific inhibitors.[38,39] The most prominent feature of the S1 pocket, which is located in the entrance funnel of GCPII, is the presence of a positively charged arginine patch and electrostatic interactions between arginine guanidinium groups and negatively charged P1 functionalities of inhibitors contribute markedly to their affinity towards GCPII.[38,40] In addition, the 'S1 hydrophobic accessory pocket' and the arene-binding site were identified as important structural features that could be used in the design of high affinity GCPII-specific probes.[41] Here, we determine and analyze the X-ray crystal structure of GCPII in complex with a carborane-containing ligand, and further discuss the interaction between the carborane-based inhibitor and the GCPII protein.

Since 2-(phosphonomethyl)pentanedioic acid (2-PMPA) was published as a GCPII inhibitor for the first time in 1996, a great number of GCPII inhibitors have been reported.[42] Based on functional groups that interact with zinc ions in the active site, GCPII inhibitors are largely classified into phosphonate-, urea-, and thiol-based subclasses. Among urea-based GCPII inhibitors, DCIBzL (Fig. 1) exhibited unique binding mode in the active site of GCPII. The additional S1 accessory pocket with its maximum observed size of 7 Å × 8.5 Å × 9 Å could accommodate the 4-iodophenyl group of DCIBzL, thus contributing to its extremely high affinity for GCPII.[43] Structural studies suggested that this accessory pocket can have variable size, that is, defined by the concerted repositioning of the Arg536, Arg534 and Arg463 side chains. At the same time, it is not clear, whether an even bigger opening of this pocket is possible, allowing for the accommodation of even larger hydrophobic moieties. To test this hypothesis as well as to synthesize more lipophilic GCPII inhibitors than DCIBzL, we designed and synthesized two novel carborane-based GCPII inhibitors, where the *p*-iodobenzene ring of DCIBzL was replaced with a *closo o*- or *m*-carborane cluster.

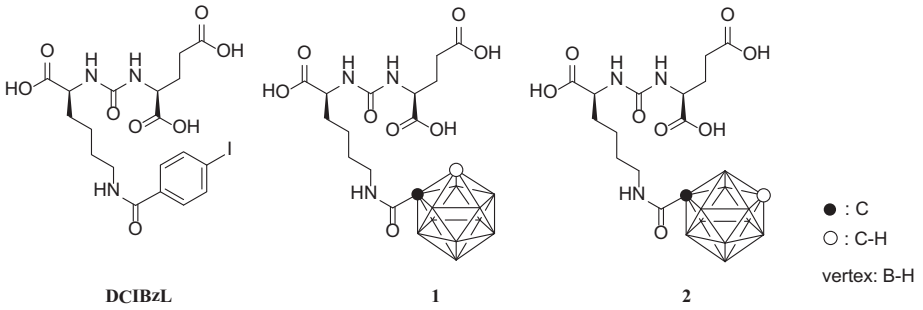


**Figure 1.** Chemical structure of DCIBzL and carborane-containing GCPII inhibitors **1** and **2**.

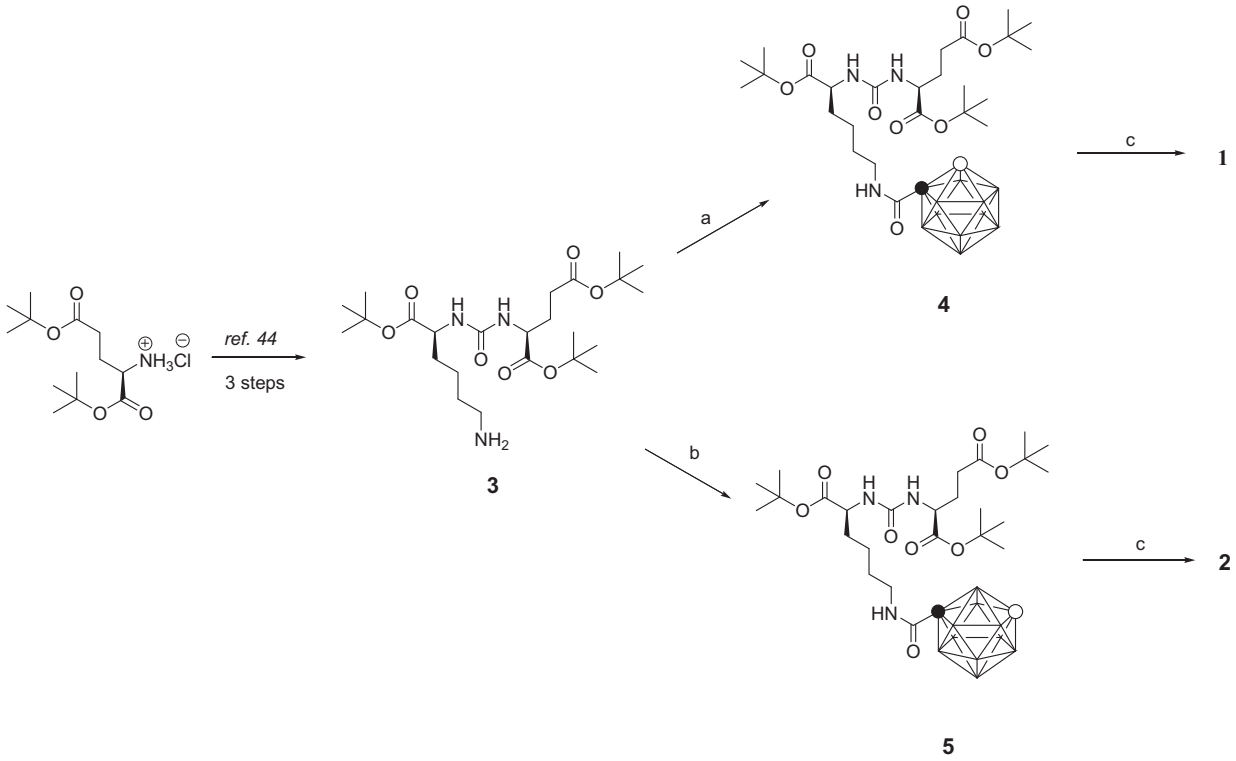


**Scheme 1.** Synthesis of carborane-containing GCPII inhibitors. Reagents and conditions: (a) 1,2-dicarba-*closo*-dodecaborane-1-carboxylic acid, HATU, TEA, DMF, rt, 12 h, 30%; (b) 1,7-dicarba-*closo*-dodecaborane-1-carboxylic acid, HATU, TEA, DMF, rt, 12 h, 25%; (c) TFA/$CH_2Cl_2$, rt, 4 h, 44% for **1** and 32% for **2**.

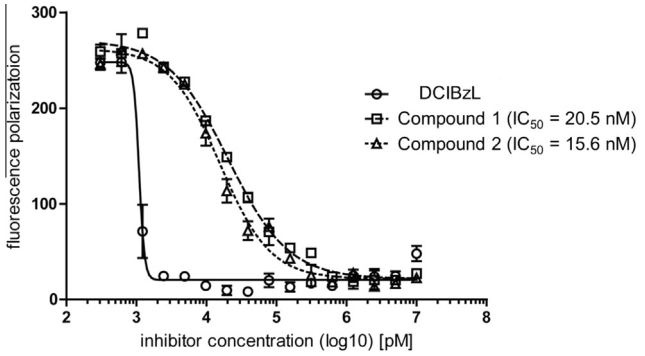


**Figure 2.** In vitro GCPII inhibition of DCIBzL and compounds **1**–**2**.

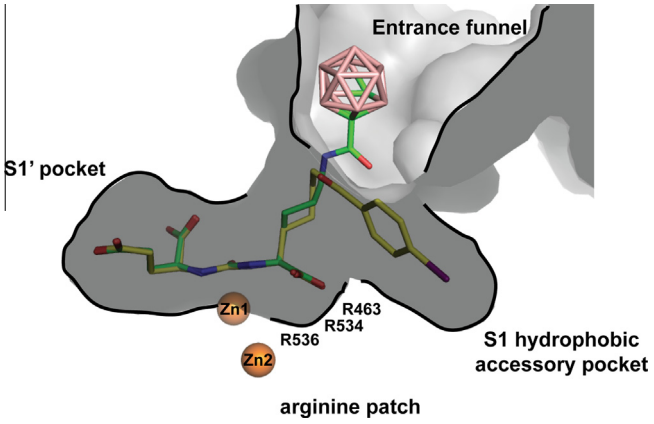


**Figure 3.** Comparison of the binding modes of DCIBzL and **1** in the internal pocket of human GCPII. Complexes of the GCPII/inhibitor were superimposed on to corresponding Cα atoms of the enzyme. Inhibitors are in stick representation, with atoms colored red (oxygen), blue (nitrogen), violet (iodine), and pink (boron). Carbon atoms are colored green (compound **1**) and yellow (DCIBzL). The zinc ions are shown as orange spheres and selected parts of GCPII are shaded gray.

The synthetic scheme for the preparation of the carborane-containing GCPII inhibitors is outlined in Scheme 1. Lys-urea-Glu scaffold **3** was synthesized from commercial protected L-lysine and L-glutamic acid in 3 steps by applying a previously published method.[44] Another starting materials, the carboxylic acids of *closo* *o*-carborane and *m*-carborane were synthesized in 1 step by using the reported synthetic procedure (see Supplementary data).[45] Briefly, treatment of *closo*-carborane with *n*-BuLi, followed by the addition of dry ice, afforded *o*-, *m*-carboranyl acid in 70% and 72% yield, respectively. Reaction of **3** with *o*- and *m*-carboranyl acids under the traditional peptide coupling conditions (HATU and DIPEA in DMF) afforded **4** and **5** in moderate yield, respectively. The low coupling yield in both cases was due to the bulkiness of *closo*-carboranyl acid which prevented the carboxylic acid group being activated by HATU. Deprotection of the *t*-butyl groups of **4** and **5** was achieved by the treatment of TFA at room temperature for 4 h to give the corresponding ligands **1** and **2**, respectively. The compounds **1** and **2** were fully analyzed by $^{1}$H NMR, $^{13}$C NMR, HPLC and ESI-MS. The ESI-MS spectra for **1** and **2** showed a $[M-H]^-$ peak at 488.3 in the negative mode with the typical isotope distribution pattern of the carborane cluster (see Supplementary data).

To compare the relative lipophilicity of **1** and **2** with DCIBzL, the retention time of the compounds were determined by reversed-phase HPLC with an isocratic mode (65% water/35% acetonitrile, 0.1% formic acid). Compounds **1** and **2** were eluted at 11.37 and 11.38 min, respectively, while DCIBzL was collected at 4.02 min (see Supplementary data). This result indicated that the *closo*-carborane cluster is more lipophilic than the 4-iodobenzene ring, resulting in

**Table 1**
Comparison of hydrogen-bonding distance between GCPII and **1** and DCIBzL

| Amino acids | Distance (Å) | |
|---|---|---|
| | DCIBzL | **1** |
| Arg210 | 2.72 | 2.66 |
| Asn257 | 2.85 | 2.96 |
| Glu424 | 3.02 | 2.92 |
| Gly518 | 2.91, 3.10 | 3.05, 3.03 |
| Asn519 | 2.92 | 2.92 |
| Arg534 | 2.92 | 2.91 |
| Arg536 | 2.84, 3.01 | 2.81, 2.98 |
| Tyr552 | 2.67, 3.13 | 2.66, 3.15 |
| Lys699 | 2.64 | 2.69 |
| Tyr700 | 2.62 | 2.55 |

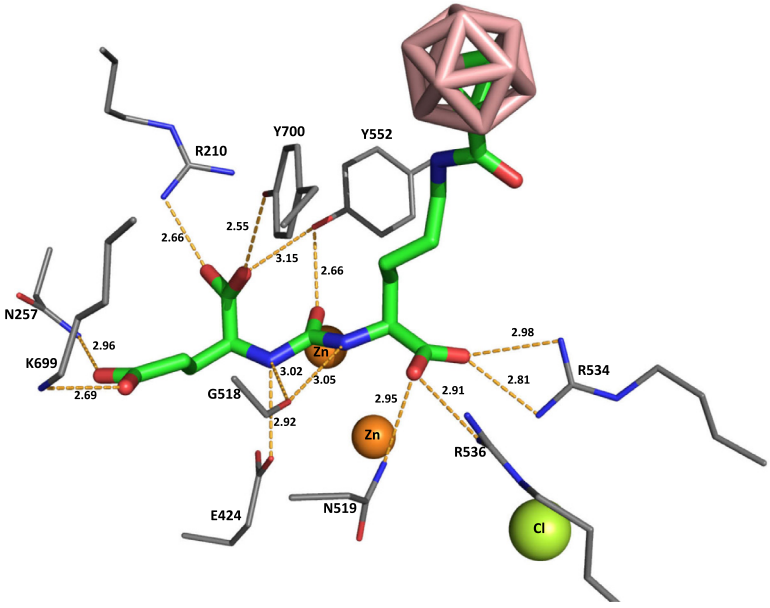


**Figure 4.** Interactions between compound **1** and key amino acid residues in the active site of GCPII.

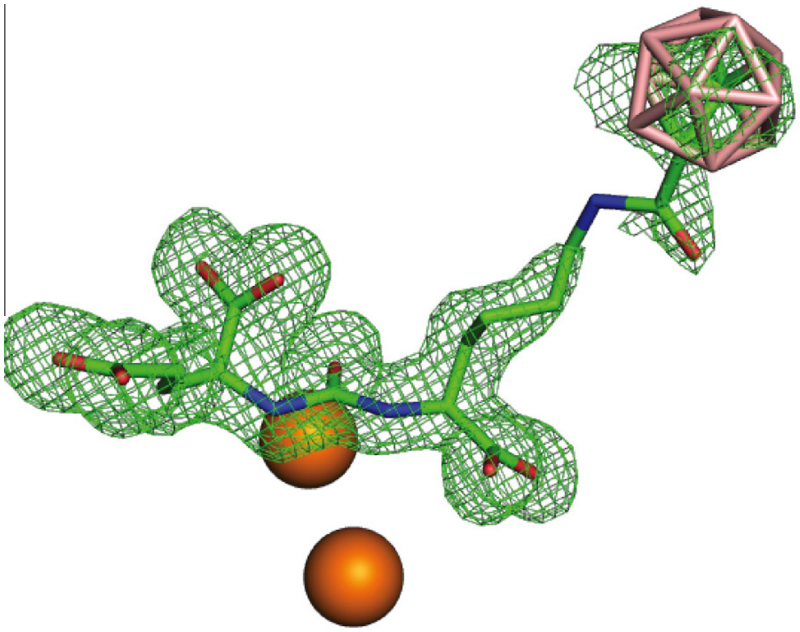

**Figure 5.** *Fo-Fc* electron density map of compound **1** in the active site of GCPII.

the delayed retention time of **1** and **2** as compared with DCIBzL. With the aim of characterizing compounds **1** and **2** as surrogates of DCIBzL, the interaction pattern between the *closo*-carborane cage and the residues lining the entrance funnel of GCPII was investigated. This data could in turn be used for the rational design of carborane-based bioactive molecules. To this end, we first determined inhibition constants for the carborane-containing inhibitors using a fluorescence polarization assay[46] and the acquired data are shown in Figure 2. The $IC_{50}$ values for compounds **1** and **2** were 20.5 nM and 15.6 nM, respectively, while the $IC_{50}$ for DCIBzL as a control was determined to be below 1 nM which is the detection limit of the assay. In fact, earlier studies using a fluorescence- or radiometry-based assay reported the $IC_{50}$ value for DCIBzL to be 0.04 nM.[43]

In order to provide a mechanistic explanation for carborane-based inhibitors, we determined the X-ray structure of the GCPII/compound **1** complex at a resolution of 1.79 Å (PDB ID: 4OME) and compared it to the structure of the GCPII/DCIBzL complex reported previously (PDB ID: 3D7H).[43] The common denominators of both inhibitors are the presence of the P1′ glutamate connected to the P1-hexanoyl linker via a urea function serving as a zinc-binding group (ZBG). Unsurprisingly, the positioning of the urea-glutamate part of inhibitors is identical for both structures and follows the 'canonical' interaction pattern within the S1′ pocket and the vicinity of the active-site zinc ions (Fig. 3).

Additionally, the P1 carboxylate present in both inhibitors forms an identical set of hydrogen bonds with the guanidinium groups of Arg536 (2.8 Å and 3.0 Å), Arg534 (2.9 Å), and the amido group of the Asn519 side chain (2.9 Å) as shown in Figure 4 and summarized in Table 1. The positioning of the remaining distal parts of both inhibitors, however, differs markedly. In the case of DCIBzL, the hexanoyl linker connecting the terminal *p*-iodophenyl group to the ureido function was fully visible in the electron density map, as its conformational space is restricted by the ureido/P1 carboxylate at one side and the *p*-iodophenyl group inserted into the S1 accessory pocket at the other side, respectively.

In fact, it is the intimate contact between the terminal *p*-iodophenyl group and the residues shaping the S1 accessory pocket that contributes to the increased affinity of DCIBzL for GCPII. Conversely, the structure of GCPII/**1** suggests that the hexanoyl linker and the carborane cluster of **1** adopt several alternate conformations within the GCPII entrance funnel. The *Fo-Fc* map for this part of the inhibitor is somewhat weaker compared with the urea-glutamate part, implying the higher flexibility of the former (Fig. 5). This observation is further supported by the substantial increase in temperature factors for atoms of the hexanoyl-carborane fragment. Combined data clearly showed that the carborane cluster cannot engage the S1 accessory pocket similarly to the *p*-iodophenyl group of DCIBzL due to the steric bulkiness of the carborane cluster. Apparently, the polyhedral shape of the carborane cluster with a diameter of approximately 7.1 Å is too big to fit into the S1 accessory pocket, and the size of the pocket observed in the GCPII/DCIBzL complex is likely close to its maximum volume and cannot be further enlarged to accommodate bigger functionalities. The absence of cation–π stacking interactions between the carborane cage and the GCPII residues in the S1 accessory pocket thus explains the decreased affinity of compound **1** compared with DCIBzL. However, the major advantage of the carborane cluster not being buried within the GCPII structure is the fact that its positioning and orientation enables the cage to be further modified to the halogenated cluster labelled with $^{76}Br$, $^{125}I$, or $^{131}I$ for imaging or therapy.[47]

In summary, we designed and synthesized novel carborane-containing urea-based inhibitors of GCPII. The X-ray crystal structure of GCPII in complex with the carborane-based inhibitor was determined at 1.79 Å resolution. As the bulky *closo*-carborane cluster is located in the spacious entrance funnel region of GCPII, the current carborane-containing compounds can be further structurally modified to identify promising lead structures of novel GCPII inhibitors.

## Acknowledgements

We thank J. Cerny and G. Murshudov for their help with the preparation of coordinate and restrains library files. C.B. acknowledges support from the Czech Science Foundation (Grant No 301/12/1513). Z.N. acknowledges support from the program "Biotechnological expert in structural biology and gene expression" (Reg #: CZ.1.07/2.3.00/30.0045). The use of MX 14.2 was in part funded by the Helmholtz-Zentrum Berlin and

BioStruct-X (Grant agreement N°283570). This publication is supported by the project BIOCEV (CZ.1.05/1.1.00/02.0109) from the ERDF. Y.B. acknowledges support from the National Research Foundation of Korea (2012R1A1A1010000, 2014R1A1A2056522 and 2014R1A4A1007304).

## Supplementary data

Supplementary data (experimental procedures and analytical data of final compounds **1**–**2** and intermediates **4**–**5**) associated with this article can be found, in the online version, at http://dx.doi.org/10.1016/j.bmcl.2015.09.062.

## References and notes

1. Ferrer-Ugalde, A.; Gonzalez-Campo, A.; Vinas, C.; Rodriguez-Romero, J.; Santillan, R.; Farfan, N.; Sillanpaa, R.; Sousa-Pedrares, A.; Nunez, R.; Teixidor, F. *Chem. Eur. J.* **2014**, *20*, 9940.
2. Bae, H. J.; Kim, H.; Lee, K. M.; Kim, T.; Lee, Y. S.; Do, Y.; Lee, M. H. *Dalton Trans.* **2014**, *43*, 4978.
3. Cansu-Ergun, E. G.; Cihaner, A. *Mater. Chem. Phys.* **2013**, *143*, 387.
4. Wee, K. R.; Cho, Y. J.; Song, J. K.; Kang, S. O. *Angew. Chem., Int. Ed.* **2013**, *52*, 9682.
5. Zhu, L.; Lv, W.; Liu, S. J.; Yan, H.; Zhao, Q.; Huang, W. *Chem. Commun.* **2013**, 10638.
6. Pasquale, F. L.; Liu, J.; Dowben, P. A.; Kelber, J. A. *Mater. Chem. Phys.* **2012**, *133*, 901.
7. Heber, E. M.; Hawthorne, M. F.; Kueffer, P. J.; Garabalino, M. A.; Thorp, S. I.; Pozzi, E. C. C.; Hughes, A. M.; Maitz, C. A.; Jalisatgi, S. S.; Nigg, D. W.; Curotto, P.; Trivillin, V. A.; Schwint, A. E. *Proc. Natl. Acad. Sci. U.S.A.* **2014**, *111*, 16077.
8. Stengl, V.; Bakardjieva, S.; Bakardjiev, M.; Stibr, B.; Kormunda, M. *Carbon* **2014**, *67*, 336.
9. Alberti, D.; Toppino, A.; Crich, S. G.; Meraldi, C.; Prandi, C.; Protti, N.; Bortolussi, S.; Altieri, S.; Aime, S.; Deagostino, A. *Org. Biomol. Chem.* **2014**, *12*, 2457.
10. Mitin, V. N.; Kulakov, V. N.; Khokhlov, V. F.; Sheino, I. N.; Arnopolskaya, A. M.; Kozlovskaya, N. G.; Zaitsev, K. N.; Portnov, A. A. *Appl. Radiat. Isotopes* **2009**, *67*, S299.
11. Snajdr, I.; Janousek, Z.; Takagaki, M.; Cisarova, I.; Hosmane, N. S.; Kotora, M. *Eur. J. Med. Chem.* **2014**, *83*, 389.
12. Satapathy, R.; Dash, B. P.; Bode, B. P.; Byczynski, E. A.; Hosmane, S. N.; Bux, S.; Hosmane, N. S. *Dalton Trans.* **2012**, *41*, 8982.
13. Zhu, Y. H.; Hosmane, N. S. *Future Med. Chem.* **2013**, *5*, 705.
14. Alberti, D.; Protti, N.; Toppino, A.; Deagostino, A.; Lanzardo, S.; Bortolussi, S.; Altieri, S.; Voena, C.; Chiarle, R.; Crich, S. G.; Aime, S. *Nanomed.-Nanotechnol.* **2015**, *11*, 741.
15. Agarwal, H. K.; Khalil, A.; Ishita, K.; Yang, W. L.; Nakkula, R. J.; Wu, L. C.; Ali, T.; Tiwari, R.; Byun, Y.; Barth, R. F.; Tjarks, W. *Eur. J. Med. Chem.* **2015**, *100*, 197.
16. Grimes, R. N. *Dalton Trans.* **2015**, *44*, 5939.
17. Bednarska, K.; Olejniczak, A. B.; Klink, M.; Sulowska, Z.; Lesnikowski, Z. J. *Bioorg. Med. Chem. Lett.* **2014**, *24*, 3073.
18. Nakamura, H.; Yasui, Y.; Ban, H. S. *J. Organomet. Chem.* **2013**, *747*, 189.
19. Nakamura, H.; Tasaki, L.; Kanoh, D.; Sato, S.; Ban, H. S. *Dalton Trans.* **2014**, *43*, 4941.
20. Issa, F.; Kassiou, M.; Rendina, L. M. *Chem. Rev.* **2011**, *111*, 5701.
21. Lee, M. W.; Sevryugina, Y. V.; Khan, A.; Ye, S. Q. *J. Med. Chem.* **2012**, *55*, 7290.
22. Austin, C. J. D.; Kahlert, J.; Issa, F.; Reed, J. H.; Smith, J. R.; Ioppolo, J. A.; Ong, J. A.; Jamie, J. F.; Hibbs, D.; Rendina, L. M. *Dalton Trans.* **2014**, *43*, 10719.
23. Fujii, S.; Sekine, R.; Kano, A.; Masuno, H.; Songkram, C.; Kawachi, E.; Hirano, T.; Tanatani, A.; Kagechika, H. *Bioorg. Med. Chem.* **2014**, *22*, 5891.
24. Fujii, S.; Nakano, E.; Yanagida, N.; Mori, S.; Masuno, H.; Kagechika, H. *Bioorg. Med. Chem.* **2014**, *22*, 5329.
25. Fujii, S.; Yamada, A.; Nakano, E.; Takeuchi, Y.; Mori, S.; Masuno, H.; Kagechika, H. *Eur. J. Med. Chem.* **2014**, *84*, 264.
26. Ohta, K.; Ogawa, T.; Kaise, A.; Endo, Y. *Bioorg. Med. Chem. Lett.* **2013**, *23*, 6555.
27. Fujii, S.; Yamada, A.; Tomita, K.; Nagano, M.; Goto, T.; Ohta, K.; Harayama, T.; Endo, Y.; Kagechika, H. *MedChemComm* **2011**, *2*, 877.
28. Rahn, K. A.; Slusher, B. S.; Kaplin, A. I. *Curr. Med. Chem.* **2012**, *19*, 1335.
29. Osborne, J.; Akhtar, N. H.; Vallabhajosula, S.; Nikolopoulou, A.; Maresca, K. P.; Hillier, S. M.; Joyal, J. L.; Crummet, R.; Armor, T.; Tagawa, S. T.; Nanus, D. M.; Goldsmith, S. J.; Babich, J. W. *J. Clin. Oncol.* **2012**, 30.
30. Graham, K.; Lesche, R.; Gromov, A. V.; Bohnke, N.; Schafer, M.; Hassfeld, J.; Dinkelborg, L.; Kettschau, G. *J. Med. Chem.* **2012**, *55*, 9510.
31. Banerjee, S. R.; Pullambhatla, M.; Byun, Y.; Nimmagadda, S.; Green, G.; Fox, J. J.; Horti, A.; Mease, R. C.; Pomper, M. G. *J. Med. Chem.* **2010**, *53*, 5333.
32. Banerjee, S. R.; Foss, C. A.; Castanares, M.; Mease, R. C.; Byun, Y.; Fox, J. J.; Hilton, J.; Lupold, S. E.; Kozikowski, A. P.; Pomper, M. G. *J. Med. Chem.* **2008**, *51*, 4504.
33. Reynolds, R. C.; Campbell, S. R.; Fairchild, R. G.; Kisliuk, R. L.; Micca, P. L.; Queener, S. F.; Riordan, J. M.; Sedwick, W. D.; Waud, W. R.; Leung, A. K.; Dixon, R. W.; Suling, W. J.; Borhani, D. W. *J. Med. Chem.* **2007**, *50*, 3283.
34. Cigler, P.; Kozisek, M.; Rezacova, P.; Brynda, J.; Otwinowski, Z.; Pokorna, J.; Plesek, J.; Gruner, B.; Doleckova-Maresova, L.; Masa, M.; Sedlacek, J.; Bodem, J.; Krausslich, H. G.; Kral, V.; Konvalinka, J. *Proc. Natl. Acad. Sci. U.S.A.* **2005**, *102*, 15394.
35. Fujii, S.; Masuno, H.; Taoda, Y.; Kano, A.; Wongmayura, A.; Nakabayashi, M.; Ito, N.; Shimizu, M.; Kawachi, E.; Hirano, T.; Endo, Y.; Tanatani, A.; Kagechika, H. *J. Am. Chem. Soc.* **2011**, *133*, 20933.
36. Mader, P.; Pecina, A.; Cigler, P.; Lepsik, M.; Sicha, V.; Hobza, P.; Gruner, B.; Fanfrlik, J.; Brynda, J.; Rezacova, P. *Biomed. Res. Int.* **2014**.
37. Brynda, J.; Mader, P.; Sicha, V.; Fabry, M.; Poncova, K.; Bakardiev, M.; Gruner, B.; Cigler, P.; Rezacova, P. *Angew. Chem., Int. Ed.* **2013**, *52*, 13760.
38. Wang, H. F.; Byun, Y.; Barinka, C.; Pullambhatla, M.; Bhang, H. E. C.; Fox, J. J.; Lubkowski, J.; Mease, R. C.; Pomper, M. G. *Bioorg. Med. Chem. Lett.* **2010**, *20*, 392.
39. Pavlicek, J.; Ptacek, J.; Cerny, J.; Byun, Y.; Skultetyova, L.; Pomper, M. G.; Lubkowski, J.; Barinka, C. *Bioorg. Med. Chem. Lett.* **2014**, *24*, 2340.
40. Barinka, C.; Hlouchova, K.; Rovenska, M.; Majer, P.; Dauter, M.; Hin, N.; Ko, Y. S.; Tsukamoto, T.; Slusher, B. S.; Konvalinka, J.; Lubkowski, J. *J. Mol. Biol.* **2008**, *376*, 1438.
41. Zhang, A. X.; Murelli, R. P.; Barinka, C.; Michel, J.; Cocleaza, A.; Jorgensen, W. L.; Lubkowski, J.; Spiegel, D. A. *J. Am. Chem. Soc.* **2010**, *132*, 12711.
42. Jackson, P. F.; Cole, D. C.; Slusher, B. S.; Stetz, S. L.; Ross, L. E.; Donzanti, B. A.; Trainor, D. A. *J. Med. Chem.* **1996**, *39*, 619.
43. Barinka, C.; Byun, Y.; Dusich, C. L.; Banerjee, S. R.; Chen, Y.; Castanares, M.; Kozikowski, A. P.; Mease, R. C.; Pomper, M. G.; Lubkowski, J. *J. Med. Chem.* **2008**, *51*, 7737.
44. Maresca, K. P.; Hillier, S. M.; Femia, F. J.; Keith, D.; Barone, C.; Joyal, J. L.; Zimmerman, C. N.; Kozikowski, A. P.; Barrett, J. A.; Eckelman, W. C.; Babich, J. W. *J. Med. Chem.* **2009**, *52*, 347.
45. Kahl, S. B.; Kasar, R. A. *J. Am. Chem. Soc.* **1996**, *118*, 1223.
46. Alquicer, G.; Sedlak, D.; Byun, Y.; Pavlicek, J.; Stathis, M.; Rojas, C.; Slusher, B.; Pomper, M. G.; Bartunek, P.; Barinka, C. *J. Biomol. Screen.* **2012**, *17*, 1030.
47. El-Zaria, M. E.; Genady, A. R.; Janzen, N.; Petlura, C. I.; Vera, D. R. B.; Valliant, J. F. *Dalton Trans.* **2014**, *43*, 4950.